Enhanced biodegradation of naphthalene by *Pseudomonas* sp. consortium immobilized in calcium alginate beads

Kunal Dutta[1], Sergey Shityakov[2], Ibrahim Khalifa[3,4], Saroj Ballav[1], Debarati Jana[1], Tuhin Manna[1], Monalisha Karmakar[1], Priyanka Raul[1], Kartik Chandra Guchhait[1] and Chandradipa Ghosh[1,*]

[1]Microbiology and Immunology Laboratory, Department of Human Physiology with Community Health, Vidyasagar University, Midnapore -721102, West Bengal, India.

[2]Department of Anaesthesia and Critical Care, University of Würzburg, 97080 Würzburg, Germany.

[3]Food Technology Department, Faculty of Agriculture, 13736 Moshtohor, Benha University, Egypt.

[4]College of Food Science and Technology, Huazhong Agricultural University, Wuhan 430070, China.

** Corresponding author:*

Prof. Chandradipa Ghosh
Microbiology and Immunology Laboratory
Department of Human Physiology with Community Health
Vidyasagar University
Midnapore - 721102
West Bengal,
INDIA
Email : ch_ghosh@mail.vidyasagar.ac.in
Phone : +91 3222 276554/555/557 Extn. 450
Fax : +91 3222 275329

Kunal Dutta : orcid.org/0000-0002-0818-8787

Sergey Shityakov : orcid.org/0000-0002-6953-9771

Ibrahim Khalifa : orcid.org/0000-0002-7648-2961

Abstract

Polycyclic aromatic hydrocarbons (PAHs) belong to a group of organic pollutants widespread in nature. PAHs are known as a serious threat to living beings and their hydrophobic nature make them major contributors to groundwater contamination. Herein, naphthalene biodegradation potential by *Pseudomonas putida* strain KD10 and a blend of *Pseudomonas* sp. isolated from different petroleum refinery waste sites are reported. *Pseudomonas putida* strain KD10 and the *Pseudomonas* sp. consortium were immobilized in calcium alginate beads (CABs) and naphthalene biodegradation efficiency was studied in liquid medium with optimized pH and temperature. Additionally, naphthalene 1, 2-dioxygenase (*nah*Ac) gene sequence analysis reveals two mutated residues inside the chain A of *nah*Ac those are not seen in the vicinity of the active site. The gas-phase binding free energy (ΔG_{London}) was found to be -7.10 kcal mol^{-1} for the mutant *nah*Ac encoded by the *Pseudomonas putida* strain KD10 which closely resembles that of the wild type variant. HPLC degradation kinetics showed that KD10 biodegrades naphthalene at the rate of 79.12 mg L^{-1} day^{-1} and it was significantly elevated up to 123 mg L^{-1} day^{-1} by the immobilized *Pseudomonas* sp. consortium. The half-life ($t_{1/2}$) for naphthalene biodegradation was 3.1 days with the inhibition constant (k_i), substrate saturation constant (k_s) and maximum specific degradation rate constant (q_{max}) of 1268 mg L^{-1}, 395.5 mg L^{-1} and 0.65 h^{-1}, respectively, for the *Pseudomonas putida* strain KD10. However, the $t_{1/2}$ value was significantly reduced to 2 days along with k_i, k_s and q_{max} value of 1475 mg L^{-1}, 298.8 mg L^{-1} and 0.71 h^{-1}, respectively, for the immobilized *Pseudomonas* sp. consortium. The GC-MS data suggest that metabolites of naphthalene biodegradation by KD10 might step-into the TCA cycle via the meta-cleavage pathway of catechol biodegradation. It is concluded that naphthalene

biodegradation performance by immobilized *Pseudomonas* sp. consortium was superior to pure *Pseudomonas putida* KD10. The microbial consortium immobilization could be a useful tool for water quality management and environmental remediation.

Key words: *Pseudomonas* sp., petroleum wastes, biodegradation, cell immobilization, mutant naphthalene 1, 2-dioxygenase, rigid-flexible molecular docking.

Highlights

- Superior naphthalene biodegradation by *Pseudomonas* sp. consortium immobilized in calcium alginate beads.
- A high mutation prone amino acid stretch inside chain A of naphthalene 1, 2-dioxygenase has been identified.
- A new naphthalene biodegradation pathway by *Pseudomonas putida* strain KD10 has been proposed.

1. Introduction

Polycyclic aromatic hydrocarbons (PAHs) have long been considered as the potential hazard for living beings (Kumari et al., 2018). Several environmental agencies including US-EPA, European Union, Environment-Canada, registered PAHs as the priority pollutants that require urgent actions to clean the environment (de Gannes and Hickey, 2017; Wang et al., 2018). Physicochemical properties of PAHs makes them major contributor for soil and ground water contamination and it spread through bio-magnification, particularly in the heavily industrialized areas (Norris, 2017). According to the Environmental Health Hazard Assessment, U.S.A., naphthalene (NAP), is not safe for drinking when the concentration is more than 170 ppb (Bruce et al., 1998). Different orthodox and expensive techniques of environmental remediation, *viz.*, incineration, gasification, plasma-gasification had been substituted by green-technologies such as bioremediation, phytoremediation, nanoremediation, *etc.* (Thomé et al., 2018).

Bioremediation is considered as one of the most cost-effective and eco-friendly oil spill management technique (Wilson and Jones, 1993). However, considering the vast volume of mobile open water system, bioremediation in aquatic environment stumble upon several limiting factors such as low local concentration of the effective microorganisms, loss of active microorganisms, *etc.* (Chen et al., 2017). Conversely, cell immobilization by calcium alginate beads (CABs) is advantageous, owing to maintaining high local concentration of the effective microorganisms. In addition, this features of cell immobilization render bacterial cell membrane stability, causes minimum production cost, can be stored for future use (Bhardwaj et al., 2000), and overall can substantially improve the stability and efficiency in the bioremediation

process (Mrozik and Piotrowska-Seget, 2010; Tyagi et al., 2011). Cell immobilization using CAB is a convenient method where maximum cells remain viable and can tolerate high concentration of toxicant for a long period of time (Lee and Heo, 2000). Moreover, calcium alginate is nontoxic to the bacterial cell and it has low production cost which facilities easy reuse (Bhardwaj et al., 2000). For this reason, worldwide initiatives have been taken to improve overall biodegradation efficiency by development of microbial consortium, including optimization of other conditions like pH, temperature, *etc.* (Chen et al., 2017). Biodegradation of a toxicant (complex nutrient for bacteria) by the mixed bacterial consortium can efficiently enhance biodegradation rate (Kumari et al., 2018). Different biodegradation pathways of each individual bacterium (Dutta et al., 2018) or a metabolic intermediates of one bacteria may act as the starting material of other bacteria (Surkatti and El-Naas, 2018), or different genetic makeup (Woyke et al., 2006) or synergetic effects of different microbial species, (Ghazali et al., 2004) or by synthesising different variant of catalytic enzymes.

Microbial consortium are of different types, mainly bacteria-bacteria, bacteria-fungi (Kumar and Philip, 2006; Yamaga et al., 2010) and it can effectively enhanced the biodegradation process (Murthy and Manonmani, 2007; Vaidya et al., 2018). Moreover, it is effective because of its cooperative nature, in particular, they can combine their metabolic capabilities to utilize the common complex nutrient (Gilbert et al., 2003). Biodegradation of complex hydrocarbon mixture necessary require the cooperation of more than one bacterium, which offers broad range of diverse enzymes that finally enhance the success of the overall processes (Wongwilaiwalin et al., 2010).

The aim of the present study is to evaluate the NAP biodegradation potential of *Pseudomonas putida* strain KD10 as free cell and as immobilized in CABs. Additionally, NAP biodegradation efficiency of the *Pseudomonas* sp. consortium was studied through the cell immobilization in CABs. In the previous study morphological changes during biodegradation of NAP was first reported that indicates *Pseudomonas putida* strain KD9 decrease in size and shape from rod to sphere and their specific growth rate was also little slower (Dutta et al., 2018). Keeping this in the mind, both morphological types of the bacteria were applied. Additionally, the naphthalene 1, 2-dioxygenase (*nah*Ac) was sequenced and analysed. In this present set of study we have identified that naphthalene biodegradation performance by immobilized *Pseudomonas* sp. consortium is superior than that of individual free or immobilized *Pseudomonas putida* strain. Further, a common mutation prone amino acid stretch in chain of A of the naphthalene 1, 2-dioxygenase have been identified. In addition, the intra and interspecies comparison of the naphthalene 1, 2-dioxygenase suggested sequence dissimilarity among different species and in few same bacterial species. Moreover, the GCMS based metabolite analysis suggested *Pseudomonas putida* KD10 reaches TCA cycle via D-gluconic acid and it follows meta-cleavage of catechol biodegradation. We apprehend that, consortium in immobilized form may give rise to efficient models for biodegradation.

2. Materials and methods

2.1. Chemicals

Naphthalene was purchased from Sigma-Aldrich chemicals Pvt. Ltd. (USA) and all the chemicals used for the media preparation were procured from the HiMedia Laboratory (Mumbai, India) together with the GC-MS and HPLC grade solvents were from the Fisher Scientific (Mumbai, India). Sodium alginate (CAS No. 9005-38-3) of medium viscosity was purchased from Merck Pvt. Ltd. (USA).

2.2. Microorganisms, growth media, growth condition and consortium preparation

Soil samples were collected from the petroleum refinery waste sites near Indian Oil (Haldia, West Bengal, India). The enrichment isolation and strain identification was carried out according to the standard protocol described previously (Dutta et al., 2017). The carbon deficient minimum medium (CSM), with a pH of 7.1, was used to cultivate the bacteria. NAP was used as sole source of carbon and energy in carbon-deficient minimal media (CSM) with following compositions: 0.2 g L^{-1} $MgSO_4$, $7H_2O$; 0.08 g L^{-1} $Ca(NO_3)_2$, $4H_2O$; 0.005 g L^{-1} $FeSO_4$, $7H_2O$; 4.8 g L^{-1}, K_2HPO_4; 1.2 g L^{-1} KH_2PO_4. *Pseudomonas putida* strain KD6 (KX786159.1) and strain KD9 (KX786158.1) and a newly isolated *Pseudomonas putida* strain KD10 (KX786157.1) with different variant of naphthalene 1, 2-dioxygenase were used to prepare the blend of *Pseudomonas* sp. consortium. The consortium was maintained in Luria-Bertani broth at 31°C with 150 rpm in order to grow the bacterial cell in its normal size and shape. Additionally, bacterial cells were grown in CSM with naphthalene as sole source of carbon and energy to obtain altered morphological variant.

2.3. Gene sequence analysis

2.3.1. Detection of naphthalene 1, 2-dioxygenase and catechol 2, 3-dioxygenase

The conventional polymerase chain reaction (PCR) for the naphthalene 1, 2-dioxygenase (*nah*Ac) and catechol 2, 3-dioxygenase (*nah*H) using specific primers (Table S1) was performed. Additionally, PCR product of *nah*Ac was sequenced and analysed according to the methods described previously (Dutta et al., 2017).

2.3.2. Clustering and phylogenetic analysis

The evolutionary distance of naphthalene 1, 2-dioxygenase among different bacterial species was analysed using BLOSUM weighted matrix followed by pairwise distance computation using MEGA (v7.0) (Kumar et al., 2016). The distance matrix was then clustered using R programming (Team, 2013) to construct the cladogram and heatmap plot. The phylogenetic position of the isolated *Pseudomonas putida* strain KD10 was analysed using previous method (Dutta et al., 2017).

2.3.3. Rigid-flexible molecular docking

The molecular docking studies were conducted using Auto Dock (v4.2.1) (Morris et al., 1998). Briefly, the centre grid dimensions were set to 20.271×61.989×87.168 with grid spacing of 0.375 Å. The virtual screening was repeated for 10 times with the same unaltered docking parameters having 2.0 Å cluster

tolerance. Additionally, the rigid-flexible molecular docking was performed using Molecular Operation Environment (Chemical Computing Group, Montreal Inc., Canada). The latter scoring function was employed to identify most favourable docked poses and to estimate the binding affinity of the protein-ligand complexes and the non-covalent interactions were analysed using the previous method (Salentin, S., et al., 2015).

2.4. Enzyme kinetic assay

The enzyme kinetic parameters of the naphthalene 1, 2-dioxygenase $_{I250, V256}$ was conducted using cell-free extract of the *Pseudomonas putida* strain KD10, grown in 250 mL of CSM with NAP (500 mg L^{-1}) as sole source of carbon and energy as described by the standard method (Dutta et al., 2017).

2.4. Detection of solvent efflux pumps system

The solvent efflux pump system (*srp*ABC) was amplified using conventional polymerase chain reaction in a thermal cycler (Mastercycler® nexus gradient, Eppendrof, (Germany) using the genomic DNA of the KD10 as template and forward, reverse primers (Table S1). Standard reaction mixtures were prepared by the procedures described previously (Dutta et al., 2018).

2.5. *Cell immobilization*

2.5.1. Cell immobilization in calcium alginate beads

Individual bacterial cell and *Pseudomonas* sp. consortium were immobilized according to the standard protocol described previously (Daâssi et al., 2014). Briefly as, sodium alginate was dissolved in 0.9 wt. % NaCl (1 gm in 40 mL 0.9 wt. % NaCl) for 24 h and sterilized by autoclaving (121°C for 15 min). Two grams of bacterial cell mass was added to 8 ml of NaCl solution and again added to the sterile alginate solution. The mixture was then gently vortex for complete homogenization. The mixture was then extruded drop wise through a hypodermic syringe into chilled sterile $CaCl_2$ solution (Figure 2). The beads were hardened in the same solution at room temperature with gently stirring for 1 h. Finally, the beads were washed several times with 0.9 wt. % NaCl to remove excess calcium ions and free cells. The beads had an average diameter of 0.5 mm and stored at 4°C. Sterile beads (without microorganisms) were used to monitor the abiotic loss of NAP. Sodium alginate of medium viscosity (≥2,000 cP) was used to prepare the calcium alginate beads (CABs).

2.5.2. Cell viability count

The viable cell enumeration in the CABs was performed by using previous protocol (Usha et al., 2010). In brief, CABs was washed in saline and keep submerged for 10 min (for saline soaking). Following soaking, the CABs were shaken with glass beads for 15 min and 1 g CABs were homogenized in 9 ml saline. The saline was then used for viable cell enumeration onto a nutrient agar plate. Plating was done with this

treated saline by series dilution method upto to 10^{-5} dilutions on nutrient agar plates. Plating was also done for the initial CFU count. For every dilution, 10 µl of the solution was plated. Plating was done by the pour plate method. Plates were incubated at 37°C for 24 h. (Jain and Pradeep, 2005).

2.6. Scanning electron microscopic (SEM) study

Samples for the SEM analysis were prepared by the protocol described elsewhere (Dutta et al., 2018). The dried samples were coated in sputter coater (Quorum-SC7620) under vacuum with a thin gold layer right before SEM analysis using a scanning electron microscope (Zeiss, EVO 18, Germany) with an accelerating voltage of 5 kV.

2.7. Biodegradation kinetics

2.7.1. Biodegradation of naphthalene in liquid medium

Naphthalene biodegradation study was conducted by the protocol described previously (Dutta et al., 2017). The conical flasks were incubated at 31°C with 150 rpm and uninoculated conical flask were used as control. Culture medium was collected at regular interval of 72 h for degradation and growth kinetic study. Additionally, the effect of initial concentration of naphthalene (150-2500 mg L^{-1}) was studied with different immobilized systems.

2.7.2. Chemical analysis

NAP biodegradation were analysed by using the 1260 infinity series (Agilent, Santa Clara, CA, USA) HPLC system equipped with Zorbax SB-C18 reversed-phase column (4.6 × 12.5 mm, 5 µm). The NAP concentration analysis was conducted using isocratic elution conditions with the mobile phase 80:20 (v/v) methanol: water at a flow rate of 1 ml min^{-1}. The detection was performed at 254 nm according to the protocol described in the literature (Dutta et al., 2017). The metabolic intermediates of NAP biodegradation were analyzed using the GC-MS system (GC Trace GC Ultra, MS-Polarisq, Thermo Scientific India Pvt. Ltd) equipped with a capillary column (TR-WaxMS, 30 m × 0.25 mm [ID] × 0.25 µm film thickness) by the protocol described elsewhere (Dutta et al., 2017). The entire analysis was performed in electron ionization, at full scan mode. The metabolite identification was based on the mass spectra comparison using the NIST Mass Spectral library (v2.0, 2008).

2.8. Data analysis

The first-order degradation kinetics model was used to estimate the residual naphthalene in CSM using equations 1, the algorithms as expressed determine the half-life ($t_{1/2}$) values of NAP in CSM. The substrate inhibition kinetic parameters were calculated using equation 2.

$$C_t = C_0 \times e^{-kt} \quad [1]$$

$$q = q_{max} \frac{S}{K_s + S + {S^2}/{K_i}}$$

The effect of SCS on growth pattern was measured by calculating the difference in optical density at 600_{nm} and expressed it by slight extension (Equation 4) the Gomperz's sigmoid growth fit equation (Equation 3).

$$y = ae^{-\exp(-k\,(x-x_c))} \quad [3]$$

$$\Delta X_c = X_{c2} - X_{c1} \quad [4]$$

The growth pattern change by SCS was considered as CFU shift (Equation 5). Where, X_{c2} = Optical density at X_{c2} and X_{c1} = Optical density at X_{c1}. NAP biodegradation was enhanced by 0.5 gm. % sucrose supplementation with CFU $_{shift}$ of 4.4 x 10^8 (Figure 1).

$$CFU_{shift} = \Delta X_c \quad [5]$$

The bacterial growth kinetics were analysed by applying the Gomperz's model using Levenberg-Marquardt algorithm in Origin® 2016 (California, USA) software and the degradation kinetic by using Graphpad Prism® 6.01 (San Diego, CA, USA).

3. Results and discussion

3.1. Isolation, identification and growth patterns of NAP degrading bacterial strain

Pseudomonas putida strain KD10 was isolated from petroleum refinery waste with its distinguished colony morphology (Figure S1a, b) on CSM agar plate after the conventional enrichment isolation protocol. The PCR product of 16S rRNA gene of the isolated strain was sequenced and deposited at NCBI (https://www.ncbi.nlm.nih.gov/) under the GenBank accession number KX786157.1. Multiple sequence alignment (MSA) followed by phylogenetic assessment suggested that the strain is belongs to the *Pseudomonas putida* group and it showed 99% sequence similarity with the previously deposited sequences of *Pseudomonas putida* (Figure S2).

NAP biodegradation property of the *Pseudomonas putida* KD10 was preliminary confirmed by the catechol test (Figure S1C) followed by growth pattern analysis in CSM with NAP as sole source of carbon and energy. Additionally, growth pattern with 0.5 gm % sucrose as a secondary carbon supplement (SCS) was compared with growth patterns in non-supplemented growth media. The Gompertz's model fit (Equation 3) was used to analyse the growth curve (Table S4).

3.2. Pseudomonas sp. *consortium, growth pattern and NAP biodegradation*

Growth pattern of the *Pseudomonas* sp. consortium, as shown in Figure 1 was optimized at 31°C and pH 7.1 suggest a successful cooperation among these three *Pseudomonas putida* strain KD6, KD9 and KD10. Further, the growth curve model (Figure 1) indicates a significant increase of total biomass of these cell population when cultivated as consortium. The artificial microbial consortium (AMC) by the stain KD6,

KD9 and KD10 showed enhanced tolerance of the high concentration of NAP (Bhatia et al., 2018).

3.3. Gene sequence and phylogenetic analysis

The naphthalene 1, 2-dioxygenase (*nah*Ac), encoded by *Pseudomonas putida* strain KD10 have only two point mutations at I250, and V256 which replaced methionine and glycine respectively (Figure S6, 3A). In previous study, additional mutations were found in the same chain A at K200, A210, E264, M284 and N334 by replacing glutamic acid, glycine, aspartic acid, isoleucine, respectively (Dutta et al. 2017, 2018). The three dimensional structural analysis suggests that the single point mutations at 200, 210, 284 and 334 cause little structural change in comparison to the wild type variant of the *nah*Ac (Figure 3B). Conversely, the stretch of amino acid sequences at the close proximity of the active site residues exactly from 248 to 266 suggest a structural mismatch among all three mutant variants of the *nah*Ac (Figure 3B). The active site of an enzyme tends to evolve fast to attain its maximum performance and functionality in a particular environment (James and Tawfik, 2003).

The occurrence of mutation from amino acid 248 to 266 of chain A, was a common feature in all three mutant variants of *nah*Ac and this particular stretch of amino acid is very close to the active site residues (Figure 3C). This implies that the "248-266" amino acid stretch is highly prone to mutation and it may influence on the enzymatic efficiency and environmental adaptability. Thus, our study provides a new insight, which could be beneficial for rational approaches of enzyme redesigning. Naphthalene 1, 2-dioxygenase is the primary enzyme for naphthalene biodegradation (Lee et al., 2019). Further, the biodegradation performance of a bacterial strain is linked

with the three dimensional structure of the catalytic enzyme and ligand binding posture (Singh et al., 2019). Previous studies suggested alteration of a single amino acid in the catalytic domain of the enzyme caused different ligand binding postures which eventually lead to an unique biodegradation pathways (Ferraro et al., 2006). In addition, site directed mutation in the catalytic domain offers superior enzyme activity (Parales et al., 1999; Parales, 2003). The comparative analysis of binding free energy helps to comprehend the superior naphthalene biodegradation performance by the *Pseudomonas* sp. consortium, which is in fact the summative activity of all three mutant variant of naphthalene 1, 2-dioxygnease.

The evolutionary trace on the *nah*Ac among other species were studied through pairwise distance matrix analysis (Figure 4), suggests a significant intra and inter species difference among *Sphingopyxis sp.*, *Croceicoccus naphthovorans, Burkholderia multivorans, Burkholderia sp. Massilis sp. and Cycloclasticus sp.* Conversely, other *Pseudomonas* sp. particularly, *Pseudomonas benzenivorans, Pseudomonas balearica, Pseudomonas stutzeri, Pseudomonas kunmingensis, Pseudomonas frederikbergensis* have similarities in their version of *nah*Ac. A few other species such as *Xenophilusa zovorans, Ralsoniam annitolilytica,* and *Paraburkholderia aromaticivorans* does not show any significant evolutionary distance in their version of *nah*Ac (Figure 4). However, a few strain of *Burkholderria multivorans* shows similarities and some other does not (Figure 4). The source of collection of these two *Burkholderria multivorans* species may be the reason of such variation in the same species (Li et al., 2007). In a study by ~~(~~Su et al., 2016~~)~~, the epigenetic impacts on the metabolic enzymes have been suggested. Moreover, the divergence of evolutionary distances of the same enzyme between different and same bacterial species indicates thrive in a particular

microenvironment. However, further studies are needed to identify underlying cause and mechanisms for such variation.

3.4. Molecular docking

Molecular docking is a computational technique that samples small molecules as ligands and macromolecule as receptor, and this virtual screening helps to understand the theoretical best conformation of the docked molecules (Meng et al., 2011). The result depicted from the rigid body molecular docking, suggests *nah*Ac-KD10$_{I250,\ V256}$ mutant has little higher binding free energy than that of mutant *nah*Ac encoded by KD9 but little lower than the *nah*Ac mutant variant encoded by the KD6 (Table 1). Moreover, the rigid-flexible molecular docking using MOE algorithms showed *nah*Ac I_{250}, G_{256} mutant variant has ΔG_{London} of -7.1 kcal mol^{-1} and $\Delta G_{GBVI/WSA}$ of -1.68 kcal mol^{-1} and that is little higher in other two mutant versions of *nah*Ac encoded by KD6 and KD9 (Table 1). The interacting amino acid residues in the active site pocket were confined to be quite same in three mutant variants, except one variation, *i.e.*,His$_{208}$ which is located about 5.49 Å away from the bicyclic ring of NAP (Figure 3D). The altered binding free energy of the *nah*Ac-KD10$_{I250,\ V256}$ may be because of the locations of mutations in a stretch of amino acid "248-266" and His$_{208}$ as a unique interacting residue of the active site (Figure 3C). Moreover, the occurrence of mutation in an amino acid stretch "248-266" is common in KD6, KD9 and KD10 suggesting "248-266" as a common mutation prone location. In addition, the non-covalent interactions of the *nah*Ac-KD10$_{I250,\ V256}$ with naphthalene, phenanthrene and anthracene suggest that Phn 352 was common residue and His 208 is involve in π- staking with bond angle of 80.58° and 77.19° respectively for naphthalene and anthracene (Table S5).

3.5. Detection of solvent efflux system

The microenvironment and internal homeostasis of a cell is crucial for maintaining its normal cellular functionality and cell tends to adapt several strategies in order to achieve it (Blanco et al., 2016). One such adaptation strategy is the solvent efflux pump system, that control intracellular toxicity to some extent (Kusumawardhani et al., 2018). The role of *srp*ABC solvent efflux pump system in the biodegradation of PAHs are common in literature (Bugg et al., 2000). Besides the other cellular activities, *srp*ABC also assist in gaining antimicrobial resistance (Schweizer, 2003). Biodegradation studies on chlorpyrifos indicate that the intermediates formed during biodegradation, acts as antimicrobial agent to other species, meaning that the metabolic intermediates may have role on inter-species competition in a particular micro-environment to thrive in nutrient-limiting condition (Anwar et al., 2009), (Raes and Bork, 2008). Besides, the role of *srp*ABC on biodegradation enhancement process is still poorly understood. The presence of *srp*ABC in *Pseudomonas putida* strain KD10 (Figure S5) and its efficient naphthalene biodegradation property can be interlinked (Dutta et al., 2018).

3.6. Cell immobilization and viability count

The viscosity of CABs determines its efficiency of the immobilization and its performance of detoxification of environmental pollutant (Young et al., 2006). With this intention, sodium alginates with medium viscosity were chosen for further studies. The efficiency of cell immobilization in CABs was evaluated by enumeration of viable cells

(Table S3). Bacteria immobilized in CABs does not significantly lose its viable biomass after 21 days of incubation at 4°C.

3.7. NAP biodegradation studies

3.7.1 By free Pseudomonas putida strain KD10

Biodegradation kinetics of NAP (500 mg L^{-1}) by the *Pseudomonas putida* strain KD10 was first tested to determine its NAP biodegradation potential (Figure 4). It was found that, after 12 days of incubation at 31°C the amount of residual NAP reduced significantly ($p<0.05$) (Figure 5). Results are also summarised at Table 3 along with names of the immobilized systems. The first order degradation kinetic data suggest that the KD10 efficiently decompose 95.22 % NAP in CSM as sole source of carbon and energy at the end of the incubation. The values of degradation rate constant (k) and half-life ($t_{1/2}$) were found to be 0.2193 and 3.1 days with R^2 of 0.981. In previous study, 99.1 % of initial NAP was removed within 96 h by strain *Bacillus fusiformis* (BFN). However, the initial concentration was very low (50 mg L^{-1} of initial NAP) (Lin et al., 2010).

After confirmation of NAP biodegradation potential of KD10, the stain was allowed to grow in association with other two strains of *Pseudomonas putida*, namely *Pseudomonas putida* strain KD6 and *Pseudomonas putida* strain KD9 (Dutta et al., 2017; Dutta et al., 2018). These two strains were selected to develop the blend of *Pseudomonas* sp. consortium as because they were collected from different isolation points and they encode different variant of *nah*Ac and they have common optimized growth parameters (temperature 31°C and pH 7.1) (Dutta et al., 2017 & Dutta et al., 2018). In addition, *Pseudomonas putida* strain KD6 encodes a six point mutant *nah*Ac

with capability to co-degrade high concentration of NAP, phenanthrene (PHN) and pyrene (PYR), (500 mg L^{-1} each) and the stain KD9, encodes a four point mutant variant of *nah*Ac with rhamnolipid production capabilities (Dutta et al. 2018).

In the previous study, $t_{1/2}$ of NAP co-biodegradation with phenanthrene and pyrene by *Pseudomonas putida* strain KD6 was 4.1 days, which was significantly reduced to 2.2 days when bacterial cells were allowed to grow as *Pseudomonas* sp. consortium with only NAP as sole source of carbon and energy (Table 3). Further, this value was found as 2.7 days for *Pseudomonas putida* KD9, suggesting *Pseudomonas putida* strain KD6 might faces some sort of substrate inhibition by the co-presence of other complex PAHs *i.e.* PHN and PYR in the system (Jiang et al., 2018) and the cooperative nature of the *Pseudomonas* sp. consortium might help to enhance the NAP bio-utilization. Microbial consortium works several ways, *viz.*, by division of labour, cross-feeding *etc.* (Smid and Lacroix, 2013). In addition, a successful consortium could also overcome shortcomings of single bacteria (Bhatia et al., 2018) and metabolically engineered consortium serves improved functionality (Bernstein et al., 2012). However, it is a fact that, bacteria select PAH among mixed PAHs based on their structural simplicity first (Dutta et al., 2017) and the velocity could be optimized by reducing the initial concentration of the PAHs gradually according to the structural simplicity (Jiang et al., 2018).

3.7.2. By immobilised Pseudomonas sp. *consortium*

The biodegradation kinetic of NAP by individual *Pseudomonas putida* strain KD6, KD9, KD10 and *Pseudomonas* sp. consortia immobilized in CABs, depicted further enhancement of overall NAP bio-utilization (Table 3). Cell immobilization using

hydrogel, such as CAB found to be advantageous rather than free cell (Hameed and Ismail, 2018). This phenomenon may be attributable to the increased level of tightness of the cross-linked polymers of the calcium alginate beads that render bacteria adequate amount of protection from harsh environment (Chen et al., 2013). However, the free bacterial cell lacks the capabilities to degrade high initial concentration of the toxicant as because they followed the conventional growth phases (Marrot et al., 2006). In addition, exposure of free bacterial cells to the high initial concentration of toxicants may challenge them to experience shock-concentration (Zhao et al., 2006). Conversely, cells immobilized in calcium alginate beads can tolerate high concentration of the toxicant and decrease the lag phase duration (Kao et al., 2014). Moreover, the diffusion limitation natures of the CABs matrix provide a high local concentration of the cell population (Bezbaruah et al., 2009). Besides this, CABs provides a remarkable stability and reusable features that effectively reduces the production cost (Daâssi et al., 2014).

Biodegradation of NAP by immobilized *Pseudomonas* sp. consortium significantly elevated the overall NAP bio-utilization efficiency with $t_{1/2}$ and R^2 values of 2 days and 0.998, respectively suggesting experimental data well correlated to the model (Table 3). The individual cell population also displayed the improved biodegradation efficiency. However, the degradation efficiency was found maximum in case of KD6, which showed a marked reduction of NAP half-life from 4.1 days to 3.0 days when grown in CSM with NAP as common complex nutrient (Table 3). It promptly suggests that CABs facilitate KD6 optimized bio-utilization of NAP, which might be masked up by the co-presence of NAP, PHN, PYR (Jiang et al., 2018). However, further studies are required to investigate behavioural patterns of consortium with mixed PAHs.

Bacterial cell grown on CSM with naphthalene as sole source of carbon and energy showed a delayed growth rate and their total biomass was also low (Figure 1). Nevertheless, growing cells on CSM prior to immobilization in CABs provide them essential adaptation periods to the toxicant and mature them for such stress condition that was found to effective for NAP biodegradation (Table 3). Immobilized cell system was found to be useful for bioremediation after prior adaptation to the surrounding environment (Partovinia and Rasekh, 2018). However, growing cells in Luria-Bertani broth does not adapt cell adequately, and their NAP removal performance was very poor (Figure S3). Herein, in this present set of study we used sodium alginate of medium viscosity and the average size of the beads were found to be 0.5 mm (Figure. 2). The inoculum was normalized (OD600nm = 0.002) for each *Pseudomonas putida* strain in order to prepare the *Pseudomonas* sp. consortium. In aqueous medium the immobilized bacterial cell mainly on the surface were exposed to naphthalene and primarily involve in the naphthalene bio-utilization process. However, due to the micro porous feature of the calcium alginate beads, microbial cells immobilized other than surface are also participates in the bio-utilization and bio-sorption process of naphthalene. Further, with time due the mechanical force generated by shaking, a few microbial cells may release from the calcium alginate beads. However, to fuel up the cell, it is necessary to uptake naphthalene for bio-utilization through step by step intra cellular enzymatic reactions (Lin et al., 2014).

3.7.3. Effect of initial naphthalene concentration on biodegradation kinetics

The effect of different initial concentration of NAP (150 – 2500 mg L^{-1}) on degradation kinetics was evaluated with immobilized KD6, KD9, and KD10 as pure and as consortium ~~format~~ (Table S2). The results suggest cell immobilization in CABs facilitates bacteria to cope with high initial concentration of NAP (Table S2). The substrate inhibition kinetic parameters, *viz.*, the maximum specific degradation rate (q_{max}), and inhibition constant (k_i) were found to be high in case of immobilized *Pseudomonas* sp. consortium and these values were 0.707 h^{-1} and 1475 mg L^{-1} (Table S2). However, we did not found any significant change on half saturation constant (k_s), suggesting the reaction does not depend on its initial concentration and the biodegradation process follows pseudo-first order reaction kinetics.

In previous study, free *Pseudomonas putida* KD9 in CSM was capable to tolerate relatively low initial concentration of NAP with k_i value of 1107 mg L^{-1} and addition of sucrose as SCS provides quite similar potential of NAP tolerance (k_i of 1429 mg L^{-1}) with that of immobilized *Pseudomonas* sp. consortium (Dutta et al., 2018). However, 0.5 gm. % sucrose as SCS in the mobile open water system might not be beneficial for bacteria to overcome the high shock concentration of the toxicant, again suggesting cell immobilization and development of effective microbial consortium as systematic optimization of biodegradation process.

3.8. Detection metabolic end product

The metabolic pathway of NAP biodegradation that might be followed by *Pseudomonas putida* strain KD10 was elucidated through GCMS of the metabolites

(Figure S4). Major metabolites were confirmed by analysing the m/z values with reference to the NIST library (Figure S4). In the previous study the major compounds ware restricted to be salicylaldehyde, catechol, D-gluconic acid and pyruvic acid, suggesting NAP biodegradation via catechol mediated pathway (Dutta et al., 2018). However, in the present study we have detected salicylic acid as an additional metabolite (Table 4), which also heads towards the catechol mediated NAP biodegradation pathway (Heitkamp et al., 1987).

Previous studies on naphthalene biodegradation suggested that catechol step into the TCA cycle by two possible pathway one is ortho-cleavage and another is meta-cleavage pathway. Presence of catechol-2, 3-dioxygenase in *Pseudomonas putida* stain KD10 (Figure S5) suggest it follow meta-cleavage of catechol biodegradation pathway. In our present set of study D-gluconic acid was found as a metabolite of naphthalene biodegradation by *Pseudomonas putida* strain KD10. We postulate that D-gluconic acid enters in the bio-conversion of naphthalene possible from glucose as precursor (Figure 6) which finally converted to pyruvate via aldolase. D-gluconic acid have ability to induce phosphate solubilisation processes (Rodriguez et al., 2004), and seemed to inhibit fungal growth (Kaur et al., 2006). Hence, suggesting *Pseudomonas putida* KD10 have growth promoting ability (Figure 6). The metabolic intermediates such as salicylic acid, catechol was reported to have plant-growth promoting activity (Lee et al., 2010). Further, the antioxidant property of the catechol help and promotes seed germination (Schweigert et al., 2001). The presence of d-gluconic acid and its subsequent entry in TCA cycle from glucose as precursor, suggest that bacteria may able to sequestered catechol upon needs.

4. Conclusion

NAP biodegradation by free and immobilized *Pseudomonas putida* strain KD10 and *Pseudomonas* sp. consortium were studied. Biodegradation of NAP was enhanced by immobilised *Pseudomonas* sp. *consortium* and 80.1% of initial NAP (500 mg L^{-1}) was utilised after 72 h of incubation. Further, initial NAP tolerance by immobilized *Pseudomonas* sp. consortium was found to be highest (1475 mg L^{-1}) with maximum specific degradation of 0.707 h^{-1}. The sequence analysis of the naphthalene 1, 2-dioxygenase suggests a significant evolutionary distance among different microbial species and in few cases, intra-species variation was observed. Moreover, a common mutation prone amino acid stretch in all three natural *nah*Ac mutants (strain KD6, KD9 and KD10) were found at close proximity of the active site and the rigid-flexible molecular docking showed better binging free energy than that of wild-type variant of *nah*Ac. This common mutation prone amino acid stretch could aid the rational approaches of enzyme redesigning. Overall, this study summarises application of bacterial cell immobilization in calcium alginate beads and development of the microbial consortium together for enhanced NAP biodegradation. However, further studies are required for the systematic optimization of PAHs biodegradation process.

Authors Contributions

KD and CG conceive the main hypothesis. KD design, performed all experiments, and wrote the manuscript. SS, IK, SB, DJ assisted KD in some

experiments. MK, TM, PR, KCG performed the statistical analysis and wrote the manuscript. CG critically proofread and wrote the manuscript. All authors read the manuscript.

Funding

University Grant Commission (UGC) Govt. of India, New Delhi, India (Grant No. VU/Innovative/Sc/17/2015).

Acknowledgement

University Grant Commission (UGC) Govt. of India, New Delhi, India (Grant No. VU/Innovative/Sc/17/2015) is sincerely acknowledged by CG. KD acknowledges Council of Scientific and Industrial Research (CSIR), Govt. of India, New Delhi, India for Senior Research Fellowship (SRF) sanction letter no. 09/599 (0082) 2K19 EMR-Z dated: 29/03/2019.

Conflict of Interest

The authors declare that they have no conflict of interests.

References

Anwar, S., Liaquat, F., Khan, Q.M., Khalid, Z.M., and Iqbal, S. (2009). Biodegradation of chlorpyrifos and its hydrolysis product 3, 5, 6-trichloro-2-pyridinol by Bacillus pumilus strain C2A1. *Journal of Hazardous Materials* 168(1)**,** 400-405.

Bernstein, H.C., Paulson, S.D., and Carlson, R.P. (2012). Synthetic Escherichia coli consortia engineered for syntrophy demonstrate enhanced biomass productivity. *Journal of biotechnology* 157(1)**,** 159-166.

Bezbaruah, A.N., Krajangpan, S., Chisholm, B.J., Khan, E., and Bermudez, J.J.E. (2009). Entrapment of iron nanoparticles in calcium alginate beads for groundwater remediation applications. *Journal of Hazardous Materials* 166(2-3)**,** 1339-1343.

Bhardwaj, T.R., Kanwar, M., Lal, R., and Gupta, A. (2000). Natural gums and modified natural gums as sustained-release carriers. *Drug development and industrial pharmacy* 26(10)**,** 1025-1038.

Bhatia, S.K., Bhatia, R.K., Choi, Y.-K., Kan, E., Kim, Y.-G., and Yang, Y.-H. (2018). Biotechnological potential of microbial consortia and future perspectives. *Critical reviews in biotechnology* 38(8)**,** 1209-1229.

Blanco, P., Hernando-Amado, S., Reales-Calderon, J., Corona, F., Lira, F., Alcalde-Rico, M., et al. (2016). Bacterial multidrug efflux pumps: much more than antibiotic resistance determinants. *Microorganisms* 4(1)**,** 14.

Bruce, R.M., Haber, L., and McClure, P. (1998). *Toxicological Review of Naphthalene (CAS No. 91-20-3): In Support of Summary Information on the Integrated Risk Information System (IRIS).* US Environmental Protection Agency, National Center for Environmental Assessment.

Bugg, T., Foght, J.M., Pickard, M.A., and Gray, M.R. (2000). Uptake and active efflux of polycyclic aromatic hydrocarbons by Pseudomonas fluorescens LP6a. *Applied and environmental microbiology* 66(12)**,** 5387-5392.

Chen, D.-Z., Fang, J.-Y., Shao, Q., Ye, J.-X., Ouyang, D.-J., and Chen, J.-M. (2013). Biodegradation of tetrahydrofuran by Pseudomonas oleovorans DT4 immobilized in calcium alginate beads impregnated with activated carbon fiber: mass transfer effect and continuous treatment. *Bioresource technology* 139**,** 87-93.

Chen, Q., Li, J., Liu, M., Sun, H., and Bao, M. (2017). Study on the biodegradation of crude oil by free and immobilized bacterial consortium in marine environment. *PloS one* 12(3)**,** e0174445.

Daâssi, D., Rodríguez-Couto, S., Nasri, M., and Mechichi, T. (2014). Biodegradation of textile dyes by immobilized laccase from Coriolopsis gallica into Ca-alginate beads. *International Biodeterioration & Biodegradation* 90**,** 71-78.

de Gannes, V., and Hickey, W.J. (2017). "Genetic Adaptations of Bacteria for Metabolism of Polycyclic Aromatic Hydrocarbons," in *Microbial Ecotoxicology*. Springer), 133-164.

Dutta, K., Shityakov, S., Das, P.P., and Ghosh, C. (2017). Enhanced biodegradation of mixed PAHs by mutated naphthalene 1,2-dioxygenase encoded by Pseudomonas putida strain KD6 isolated from petroleum refinery waste. *3 Biotech* 7(6)**,** 365. doi: 10.1007/s13205-017-0940-1.

Dutta, K., Shityakov, S., Khalifa, I., Mal, A., Moulik, S.P., Panda, A.K., et al. (2018). Effects of secondary carbon supplement on biofilm-mediated biodegradation of naphthalene by mutated naphthalene 1, 2-dioxygenase encoded by Pseudomonas putida strain KD9. *Journal of Hazardous Materials* 357**,** 187-197. doi: https://doi.org/10.1016/j.jhazmat.2018.05.024.

Ferraro, D.J., Okerlund, A.L., Mowers, J.C., and Ramaswamy, S. (2006). Structural basis for regioselectivity and stereoselectivity of product formation by naphthalene 1, 2-dioxygenase. *Journal of Bacteriology* 188(19)**,** 6986-6994.

Ghazali, F.M., Rahman, R.N.Z.A., Salleh, A.B., and Basri, M. (2004). Biodegradation of hydrocarbons in soil by microbial consortium. *International Biodeterioration & Biodegradation* 54(1)**,** 61-67.

Gilbert, E., Walker, A., and Keasling, J. (2003). A constructed microbial consortium for biodegradation of the organophosphorus insecticide parathion. *Applied microbiology and biotechnology* 61(1)**,** 77-81.

Hameed, B.B., and Ismail, Z.Z. (2018). Decolorization, biodegradation and detoxification of reactive red azo dye using non-adapted immobilized mixed cells. *Biochemical Engineering Journal* 137**,** 71-77.

Heitkamp, M.A., Freeman, J.P., and Cerniglia, C.E. (1987). Naphthalene biodegradation in environmental microcosms: estimates of degradation rates and characterization of metabolites. *Applied and environmental microbiology* 53(1)**,** 129-136.

James, L.C., and Tawfik, D.S. (2003). Conformational diversity and protein evolution–a 60-year-old hypothesis revisited. *Trends in biochemical sciences* 28(7)**,** 361-368.

Jiang, Y., Zhang, Z., and Zhang, X. (2018). Co-biodegradation of pyrene and other PAHs by the bacterium Acinetobacter johnsonii. *Ecotoxicology and environmental safety* 163**,** 465-470.

Kao, P.-M., Hsu, B.-M., Huang, K.-H., Tao, C.-W., Chang, C.-M., and Ji, W.-T. (2014). Biohydrogen production by immobilized co-culture of Clostridium butyricum and Rhodopseudomonas palustris. *Energy Procedia* 61**,** 834-837.

Kaur, R., Macleod, J., Foley, W., and Nayudu, M. (2006). Gluconic acid: An antifungal agent produced by Pseudomonas species in biological control of take-all. *Phytochemistry* 67(6)**,** 595-604.

Kumar, M., and Philip, L. (2006). Enrichment and isolation of a mixed bacterial culture for complete mineralization of endosulfan. *Journal of environmental science and health Part B* 41(1)**,** 81-96.

Kumar, S., Stecher, G., and Tamura, K. (2016). MEGA7: molecular evolutionary genetics analysis version 7.0 for bigger datasets. *Molecular biology and evolution* 33(7)**,** 1870-1874.

Kumari, S., Regar, R.K., and Manickam, N. (2018). Improved polycyclic aromatic hydrocarbon degradation in a crude oil by individual and a consortium of bacteria. *Bioresource technology* 254**,** 174-179.

Kusumawardhani, H., Hosseini, R., and de Winde, J.H. (2018). Solvent tolerance in bacteria: fulfilling the promise of the Biotech Era? *Trends in biotechnology*.

Lee, K.-Y., and Heo, T.-R. (2000). Survival of Bifidobacterium longumImmobilized in calcium alginate beads in simulated gastric juices and bile salt solution. *Applied and environmental microbiology* 66(2)**,** 869-873.

Lee, S., Kim, S.G., and Park, C.M. (2010). Salicylic acid promotes seed germination under high salinity by modulating antioxidant activity in Arabidopsis. *New Phytologist* 188(2)**,** 626-637.

Lee, Y., Lee, Y., and Jeon, C.O. (2019). Biodegradation of naphthalene, BTEX, and aliphatic hydrocarbons by Paraburkholderia aromaticivorans BN5 isolated from petroleum-contaminated soil. *Scientific reports* 9.

Li, X., He, J., and Li, S. (2007). Isolation of a chlorpyrifos-degrading bacterium, Sphingomonas sp. strain Dsp-2, and cloning of the mpd gene. *Research in Microbiology* 158(2)**,** 143-149.

Lin, C., Gan, L., and Chen, Z.-L. (2010). Biodegradation of naphthalene by strain Bacillus fusiformis (BFN). *Journal of Hazardous Materials* 182(1-3)**,** 771-777.

Lin, C., Gan, L., Chen, Z., Megharaj, M., and Naidu, R. (2014). Biodegradation of naphthalene using a functional biomaterial based on immobilized Bacillus fusiformis (BFN). *Biochemical Engineering Journal* 90**,** 1-7.

Marrot, B., Barrios-Martinez, A., Moulin, P., and Roche, N. (2006). Biodegradation of high phenol concentration by activated sludge in an immersed membrane bioreactor. *Biochemical Engineering Journal* 30(2)**,** 174-183.

Meng, X.-Y., Zhang, H.-X., Mezei, M., and Cui, M. (2011). Molecular docking: a powerful approach for structure-based drug discovery. *Current computer-aided drug design* 7(2)**,** 146-157.

Morris, G.M., Goodsell, D.S., Halliday, R.S., Huey, R., Hart, W.E., Belew, R.K., et al. (1998). Automated docking using a Lamarckian genetic algorithm and an empirical binding free energy function. *Journal of computational chemistry* 19(14)**,** 1639-1662.

Mrozik, A., and Piotrowska-Seget, Z. (2010). Bioaugmentation as a strategy for cleaning up of soils contaminated with aromatic compounds. *Microbiological research* 165(5)**,** 363-375.

Murthy, H.R., and Manonmani, H. (2007). Aerobic degradation of technical hexachlorocyclohexane by a defined microbial consortium. *Journal of Hazardous Materials* 149(1)**,** 18-25.

Norris, R.D. (2017). "In-situ bioremediation of soils and ground water contaminated with petroleum hydrocarbons," in *Handbook of Bioremediation (1993)*. CRC Press), 17-38.

Parales, R.E. (2003). The role of active-site residues in naphthalene dioxygenase. *Journal of Industrial Microbiology and Biotechnology* 30(5)**,** 271-278.

Parales, R.E., Parales, J.V., and Gibson, D.T. (1999). Aspartate 205 in the catalytic domain of naphthalene dioxygenase is essential for activity. *Journal of Bacteriology* 181(6)**,** 1831-1837.

Partovinia, A., and Rasekh, B. (2018). Review of the immobilized microbial cell systems for bioremediation of petroleum hydrocarbons polluted environments. *Critical Reviews in Environmental Science and Technology* 48(1)**,** 1-38.

Raes, J., and Bork, P. (2008). Molecular eco-systems biology: towards an understanding of community function. *Nature Reviews Microbiology* 6(9)**,** 693.

Rodriguez, H., Gonzalez, T., Goire, I., and Bashan, Y. (2004). Gluconic acid production and phosphate solubilization by the plant growth-promoting bacterium Azospirillum spp. *Naturwissenschaften* 91(11)**,** 552-555.

Schweigert, N., Zehnder, A.J., and Eggen, R.I. (2001). Chemical properties of catechols and their molecular modes of toxic action in cells, from microorganisms to mammals: minireview. *Environmental microbiology* 3(2)**,** 81-91.

Schweizer, H.P. (2003). Efflux as a mechanism of resistance to antimicrobials in Pseudomonas aeruginosa and related bacteria: unanswered questions. *Genet Mol Res* 2(1)**,** 48-62.

Singh, N.S., Sharma, R., and Singh, D.K. (2019). Identification of enzyme (s) capable of degrading endosulfan and endosulfan sulfate using in silico techniques. *Enzyme and Microbial Technology* 124**,** 32-40.

Smid, E.J., and Lacroix, C. (2013). Microbe–microbe interactions in mixed culture food fermentations. *Current opinion in biotechnology* 24(2)**,** 148-154.

Su, X., Wellen, K.E., and Rabinowitz, J.D. (2016). Metabolic control of methylation and acetylation. *Current opinion in chemical biology* 30**,** 52-60.

Surkatti, R., and El-Naas, M. (2018). Competitive interference during the biodegradation of cresols. *International Journal of Environmental Science and Technology* 15(2)**,** 301-308.

Team, R.C. (2013). R: A language and environment for statistical computing.

Thomé, A., Reginatto, C., Vanzetto, G., and Braun, A.B. (Year). "Remediation Technologies Applied in Polluted Soils: New Perspectives in This Field", in: *The International Congress on Environmental Geotechnics*: Springer), 186-203.

Tyagi, M., da Fonseca, M.M.R., and de Carvalho, C.C. (2011). Bioaugmentation and biostimulation strategies to improve the effectiveness of bioremediation processes. *Biodegradation* 22(2)**,** 231-241.

Usha, M., Sanjay, M., Gaddad, S., and Shivannavar, C. (2010). Degradation of h-acid by free and immobilized cells of Alcaligenes latus. *Brazilian Journal of Microbiology* 41(4)**,** 931-945.

Vaidya, S., Devpura, N., Jain, K., and Madamwar, D. (2018). Degradation of chrysene by enriched bacterial consortium. *Frontiers in Microbiology* 9**,** 1333.

Wang, L., Zhang, S., Wang, L., Zhang, W., Shi, X., Lu, X., et al. (2018). Concentration and risk evaluation of polycyclic aromatic hydrocarbons in urban soil in the typical semi-arid city of Xi'an in Northwest China. *International journal of environmental research and public health* 15(4)**,** 607.

Wilson, S.C., and Jones, K.C. (1993). Bioremediation of soil contaminated with polynuclear aromatic hydrocarbons (PAHs): a review. *Environmental pollution* 81(3)**,** 229-249.

Wongwilaiwalin, S., Rattanachomsri, U., Laothanachareon, T., Eurwilaichitr, L., Igarashi, Y., and Champreda, V. (2010). Analysis of a thermophilic lignocellulose degrading microbial consortium and multi-species

lignocellulolytic enzyme system. *Enzyme and Microbial Technology* 47(6)**,** 283-290.

Woyke, T., Teeling, H., Ivanova, N.N., Huntemann, M., Richter, M., Gloeckner, F.O., et al. (2006). Symbiosis insights through metagenomic analysis of a microbial consortium. *Nature* 443(7114)**,** 950.

Yamaga, F., Washio, K., and Morikawa, M. (2010). Sustainable biodegradation of phenol by Acinetobacter calcoaceticus P23 isolated from the rhizosphere of duckweed Lemna aoukikusa. *Environmental science & technology* 44(16)**,** 6470-6474.

Young, C.C., Rekha, P., Lai, W.A., and Arun, A. (2006). Encapsulation of plant growth-promoting bacteria in alginate beads enriched with humic acid. *Biotechnology and bioengineering* 95(1)**,** 76-83.

Zhao, X., Wang, Y., Ye, Z., Borthwick, A.G., and Ni, J. (2006). Oil field wastewater treatment in biological aerated filter by immobilized microorganisms. *Process Biochemistry* 41(7)**,** 1475-1483.

Figure legends

Figure 1. Growth kinetic model of *Pseudomonas putida* and *Pseudomonas* sp. consortium during naphthalene biodegradation. **A.** Gompertz's growth kinetic model fit of the biodegradation of naphthalene by *Pseudomonas putida* strain KD10 and by the *Pseudomonas* sp. consortium. **B.** Effect of 0.5 gm. % sucrose supplementation on growth pattern of *Pseudomonas putida* strain KD10 and *Pseudomonas* sp. consortium.

Figure 2. Cell immobilization in calcium alginate beads (CABs) with different cell morphology of the *Pseudomonas putida* strain KD10.

Figure 3. Sequence and structure analysis of the naphthalene 1, 2-dioxygenase (*nah*Ac) encoded by *Pseudomonas putida*. **A**. The amino acid sequence of wild type and three mutant variants of the naphthalene 1, 2-dioxygenase (*nah*Ac). Mutated residues are highlighted in blue and the common mutation prone amino acid stretch is highlighted with red box. **B.** Structural mismatches among mutant variants and wild type naphthalene 1, 2-dioxygenase. Each mutated residues and its subsequent neighbour residues of all the mutant variant of naphthalene 1, 2-dioxygenase is overlaid with cartoon representation. The highlighted red circle indicates local mismatch among the mutant variant of naphthalene 1, 2-dioxygenase **C.** Different ligand binding posture of the naphthalene 1, 2-dioxygenase encoded by *Pseudomonas putida* strain KD10. Naphthalene (red), phenanthrene (cyan) and anthracene (green) binding postures with major interacting amino acid residues (left). Two-dimensional presentation of the interacting residues of *nah*Ac$_{I250, V256}$ (right). **D.** Docking pose of naphthalene 1, 2-dioxygenase (Chain A) encoded by *Pseudomonas putida* strain KD10. The four major naphthalene interacting residues and their molecular distance are labelled in black.

Figure 4. Distance matrix and cladogram of the naphthalene 1, 2-dioxygenase. The evolutionary distance of the naphthalene 1, 2-dioxygenase I_{250}, V_{255} variant encoded by *Pseudomonas putida* strain KD10 other variants by different microbial species is scaled by colour index (upper-left side).

Figure 5. Naphthalene degradation kinetics of *Pseudomonas putida* strain KD10 and *Pseudomonas* sp. consortium free and cell immobilized in calcium alginate beads.

Figure 6. Proposed pathway of naphthalene biodegradation by *Pseudomonas putida* strain KD10. Naphthalene (I), salicylic acid (II), salicylaldehyde (III), catechol (IV), pyruvate (V), glucose (VI), d-gluconic acid (VII). The grey arrow indicates alternative pathway via d-gluconic acid.

Table captions

Table 1. Summary of rigid-flexible molecular docking for the analysed mutant naphthalene 1, 2-dioxygenase encoded by different *Pseudomonas putida* strains.

Table 2. Apparent enzyme kinetic parameters of naphthalene 1, 2-dioxygenase $_{I250, V256}$ encoded by *Pseudomonas putida* strain KD10.

Table 3. Parameters of first-order biodegradation kinetics of naphthalene by different free and immobilized *Pseudomonas putida* strains.

Table 4. Major metabolite detected by GCMS analysis during naphthalene biodegradation by *Pseudomonas putida* KD10.

Supplementary section

Table S1. Nucleotide sequences used as primer in polymerase chain reactions

Table S2. Parameters of substrate inhibition kinetic model of naphthalene biodegradation by different *Pseudomonas putida* strains immobilized in calcium alginate beads.

Table S3. Enumeration of viable cell in calcium alginate beads.

Table S4. Gompertz's growth curve model fit of *Pseudomonas putida* strain KD10 and *Pseudomonas* sp. consortium.

Table S5. Major amino acid residues of mutant variant of naphthalene 1, 2-dioxygenase $_{I250, V256}$ involve in hydrophobic interaction with different ligands.

Figure S1. Colony morphology and catechol confirmatory test. **A.** Colony morphology of *Pseudomonas putida* strain KD10 after 24 h of incubation. **B.** Colony morphology of *Pseudomonas putida* strain KD10 after one week of incubation.

Figure S2. Molecular phylogenetic analysis of *Pseudomonas putida* strain KD10.

Figure S3. Effect of cell adaptation on NAP biodegradation.

Figure S4. Mass spectra of the major metabolites detected during biodegradation of naphthalene in CSM as sole source of carbon and energy by *Pseudomonas putida* KD10.

Figure S5. Agarose gel electrophoresis of PCR products of catechol 2, 3-dioxygenase (*nah*H) gene and solvent efflux pump (*srp*ABC) system.
A. Catechol 2, 3-dioxygenase (*nah*H). Lane 1 and 2 *nah*H pcr product of *Pseudomonas putida* strain KD9 and *Pseudomonas putida* strain KD10. **B.** Solvent efflux pump (*srp*ABC) system. Lane 1: *Pseudomonas aeruginoasa* ATCC 9027, Lane 2: *Pseudomonas putida* strain KD10. Lane M: 100bp DNA ladder (HiMedia, India), Lane 3: Negative control.

Figure S6. Nucleotide sequence chromatogram of the mutant naphthalene 1, 2-dioxygenase (*nah*Ac), (chain-A) encoded by *Pseudomonas putida* strain KD10.

Table 1. Summary of rigid-flexible molecular docking of naphthalene and different mutant version of naphthalene 1, 2-dioxygenase encoded by different *Pseudomonas putida* strains

ΔG*			LB[4]	IC[5]	IME[6]	VDW[7]	RMSD[c]	RMSD[r]	References
BE[1]	London[2]	GBVI/ WSA[3]							
-5.92[a]	-7.18	-4.61	-0.59	46.14	-5.92	-5.91	0.00	77.29	Dutta et al., 2017
-5.41[b]	-7.13	-4.02	-0.54	109.07	-5.41	-5.4	0.00	96.32	Dutta et al., 2019
-5.83[c]	-7.10	-1.68	-0.58	53.13	-5.83	-5.84	0.00	96.08	This study

*PubChem ligand CID 931 = Naphthalene, BE[1] = Binding free energy, [2]London free energy, [3]Generalized born volume integral/weighted surface areas, LB[4] = ligand binding, IC[5] = inhibition constant, IME[6] = Intermolecular energy, VDW[7] = Vdw hb desolv energy, RMSD[c] = Cluster RMSD, RMSD[r] = Reference RMSD. Energy unit = kcal mol^{-1}. Inhibition constant unit = µM.at 298.15 K. Naphthalene 1, 2-dioxygenase encoded by (a) *Pseudomonas putida* strain KD6, (b) *Pseudomonas putida* strain KD9 and (c) *Pseudomonas putida* strain KD10.

Table 2. Apparent enzyme kinetic parameters of naphthalene 1, 2-dioxygenase $_{I250, V256}$ encoded by *Pseudomonas putida* strain KD10

Substrate	Kinetic parameters*				
	Km (μmol mL^{-1})	Vmax (μmol min^{-1})	Kcat (s^{-1})	Kcat/Km (mL^{-1} mol^{-1} s^{-1})	R^{2**}
Naphthalene	0.867	2.474	123.72	0.142×10^{3}	0.938

*The kinetic constant were determined at 30°C and pH 7.5 using 0.5-10µM ml^{-1} substrate concentration (each) by Lineweaver–Burk plot.
** Non-liner regression between initial substrate concentration 1/[S] and degradation rate constant 1/V yielded regression equation and regression coefficient (R^2)

Table 3. Parameters of first-order biodegradation kinetics of naphthalene by different free and immobilized *Pseudomonas putida* strains

CSM	Cells immobilized in CABs			free cells			
	k (Days^{-1})	t ½ (Days^{-1})	R^2	k (Days^{-1})	t ½ (Days^{-1})	R^2	References
A	0.228±0.005	3.0±0.077	0.99	0.167±0.012	4.1±0.307	0.98	Dutta et al., 2017
B	0.312±0.014	2.2±0.102	0.93	0.252±0.019	2.7±0.193	0.99	Dutta et al., 2018
C	0.284±0.017	2.4±0.143	0.97	0.219±0.009	3.1±0.137	0.92	This study
D	0.341±0.294	2.0±0.186	0.99	0.309±0.020	2.2±0.141	0.98	This study

[#]Initial naphthalene concentration = 500 mg L^{-1}
A. *Pseudomonas putida* strain KD6, B. *Pseudomonas putida* strain KD9, C. *Pseudomonas putida* strain KD10. D. *Pseudomonas* sp. consortium.
Each figure of the table represents the mean of three replicates.

Table 4. Major metabolites detected by GCMS analysis during naphthalene biodegradation by *Pseudomonas putida* KD10

Metabolite	R_t (min)	Major ion peaks (m/z)	Suggested structure
I	9.41	64.19, 92.17, 120.21, 138.22, 169.14, 191.18, 211.10	Salicylic acid
II	15.27	65.17, 74.41, 104.73, 121.10, 122.57, 142.21, 174.80, 201.22, 249.31	Salicylaldehyde
III	18.71	64.29, 81.35, 91.61, 110.47, 131.47, 149.71	Catechol
IV	31.89	61.21, 73.44, 76.24, 104.18, 117.41, 133.27, 177.23	D-gluconic acid
V	10.47	43.21, 61.27, 71.37	Pyruvic acid

R_t = Retention time

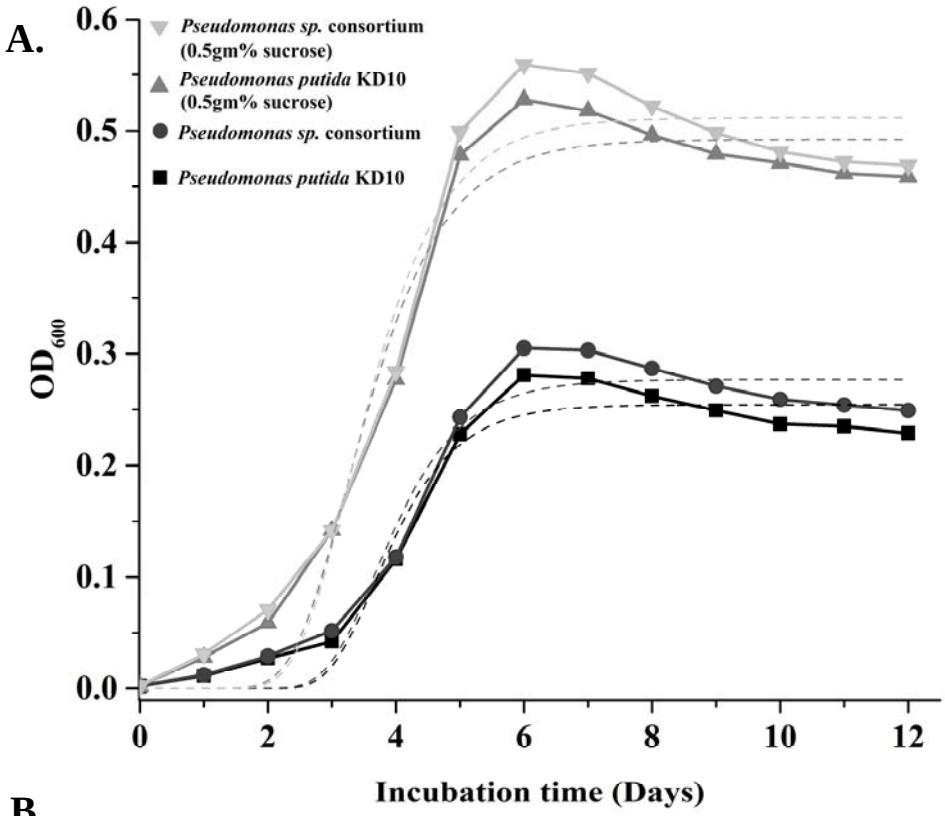
A.
Pseudomonas sp. consortium (0.5gm% sucrose)
Pseudomonas putida KD10 (0.5gm% sucrose)
Pseudomonas sp. consortium
Pseudomonas putida KD10
OD600
Incubation time (Days)

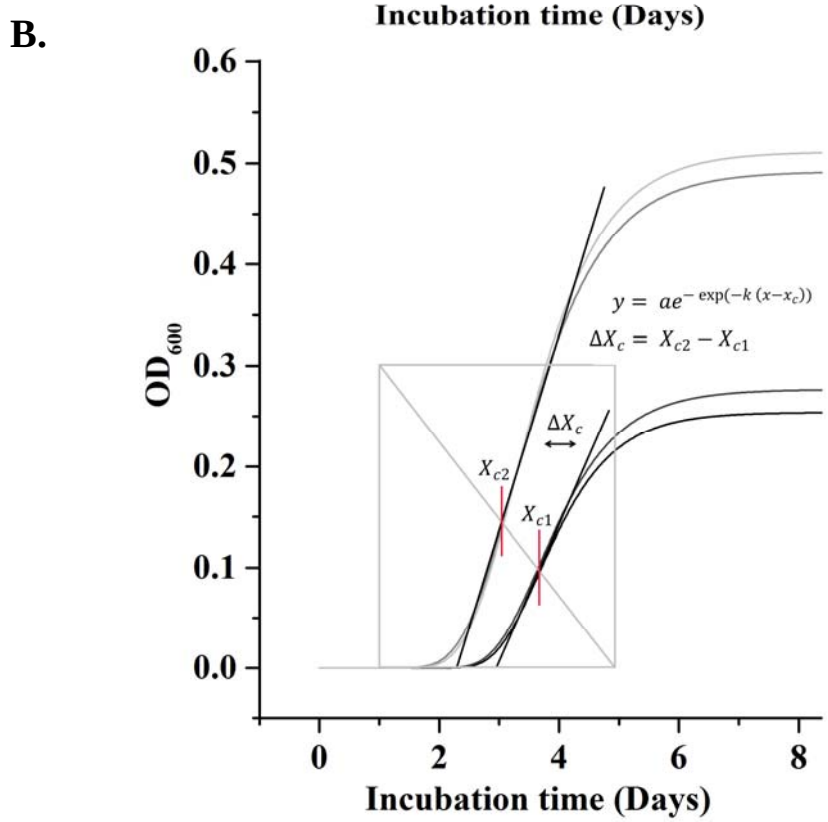
B.
$y = ae^{-\exp(-k(x-x_c))}$
$\Delta X_c = X_{c2} - X_{c1}$
ΔX_c
X_{c2}
X_{c1}
OD600
Incubation time (Days)

Figure 1.

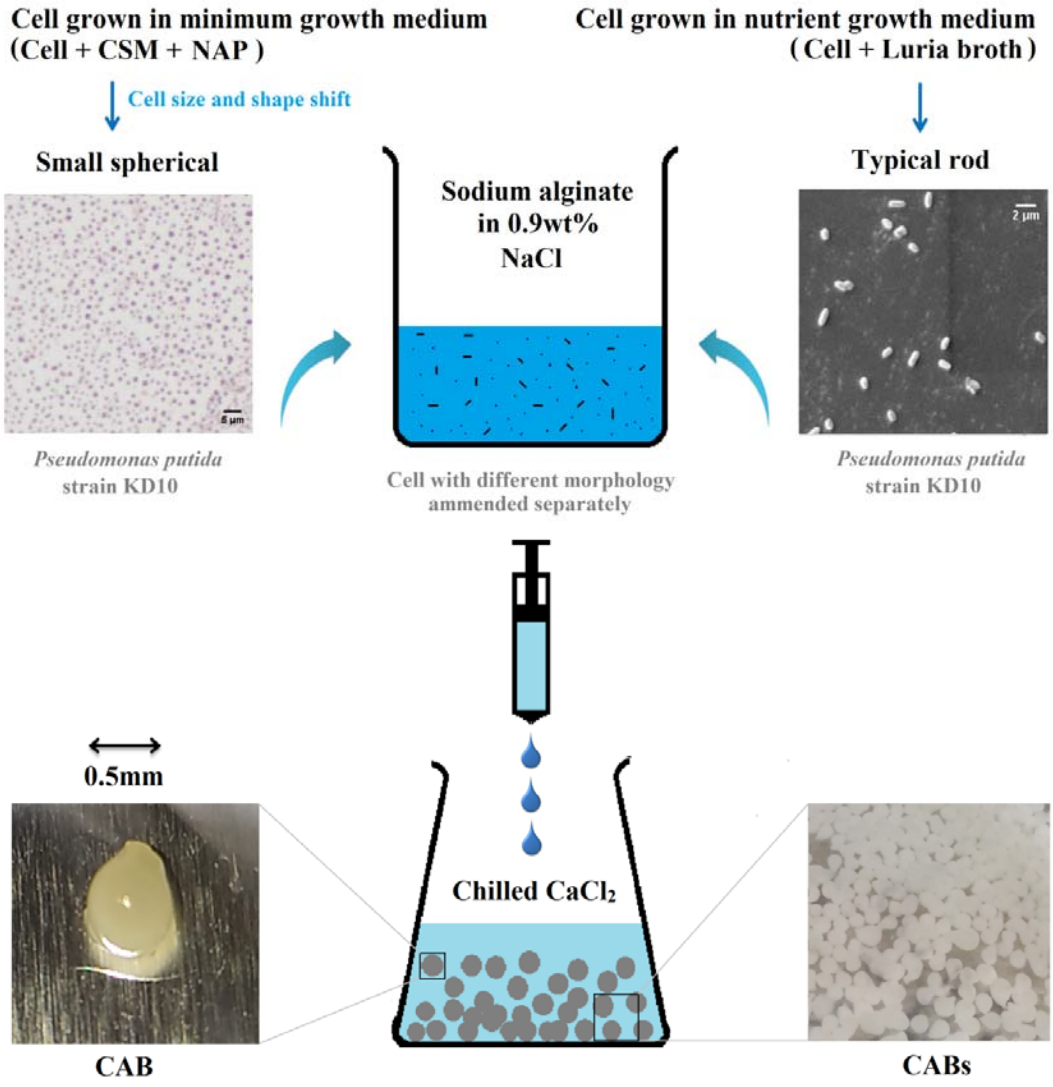
Cell grown in minimum growth medium
(Cell + CSM + NAP)
Cell grown in nutrient growth medium
(Cell + Luria broth)
Cell size and shape shift
Small spherical
Typical rod
Sodium alginate
in 0.9wt%
NaCl
2 μm
Pseudomonas putida
strain KD10
Cell with different morphology
ammended separately
Pseudomonas putida
strain KD10
0.5mm
Chilled CaCl₂
CAB
CABs

Figure 2.

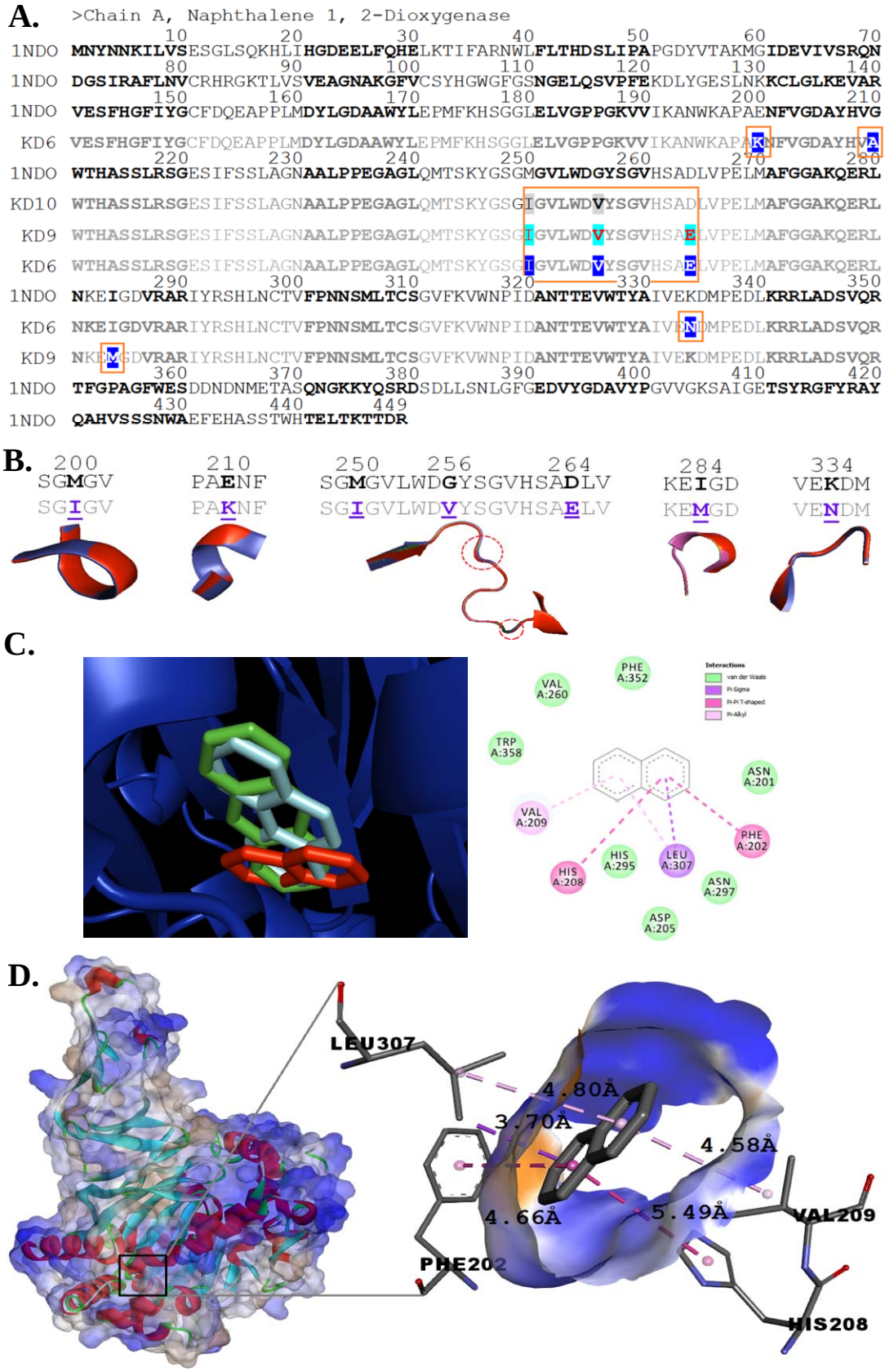

1029

Figure 3.

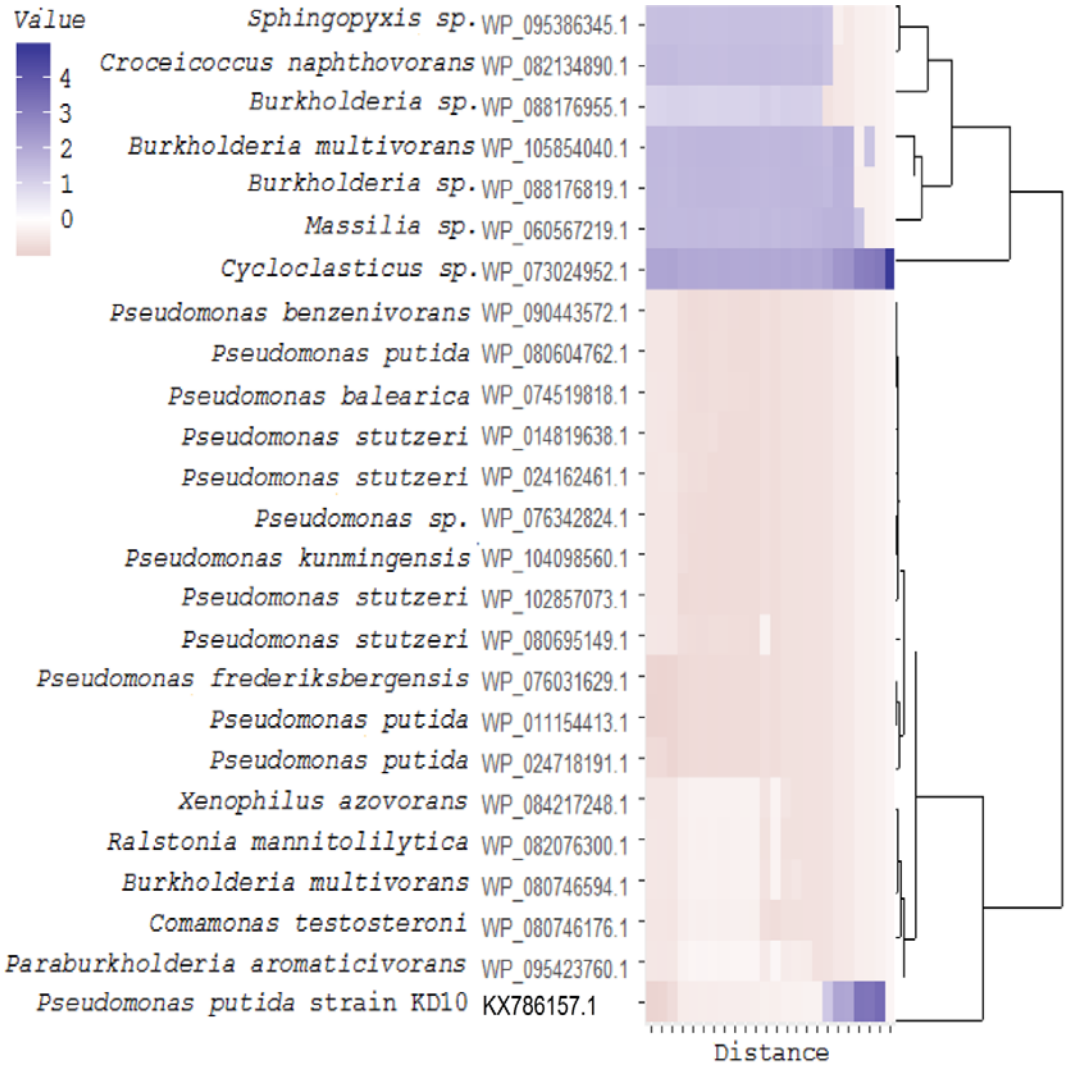
Value
4
3
2
1
0
Sphingopyxis sp. WP_095386345.1
Croceicoccus naphthovorans WP_082134890.1
Burkholderia sp. WP_088176955.1
Burkholderia multivorans WP_105854040.1
Burkholderia sp. WP_088176819.1
Massilia sp. WP_060567219.1
Cycloclasticus sp. WP_073024952.1
Pseudomonas benzenivorans WP_090443572.1
Pseudomonas putida WP_080604762.1
Pseudomonas balearica WP_074519818.1
Pseudomonas stutzeri WP_014819638.1
Pseudomonas stutzeri WP_024162461.1
Pseudomonas sp. WP_076342824.1
Pseudomonas kunmingensis WP_104098560.1
Pseudomonas stutzeri WP_102857073.1
Pseudomonas stutzeri WP_080695149.1
Pseudomonas frederiksbergensis WP_076031629.1
Pseudomonas putida WP_011154413.1
Pseudomonas putida WP_024718191.1
Xenophilus azovorans WP_084217248.1
Ralstonia mannitolilytica WP_082076300.1
Burkholderia multivorans WP_080746594.1
Comamonas testosteroni WP_080746176.1
Paraburkholderia aromaticivorans WP_095423760.1
Pseudomonas putida strain KD10 KX786157.1
Distance

Figure 4.

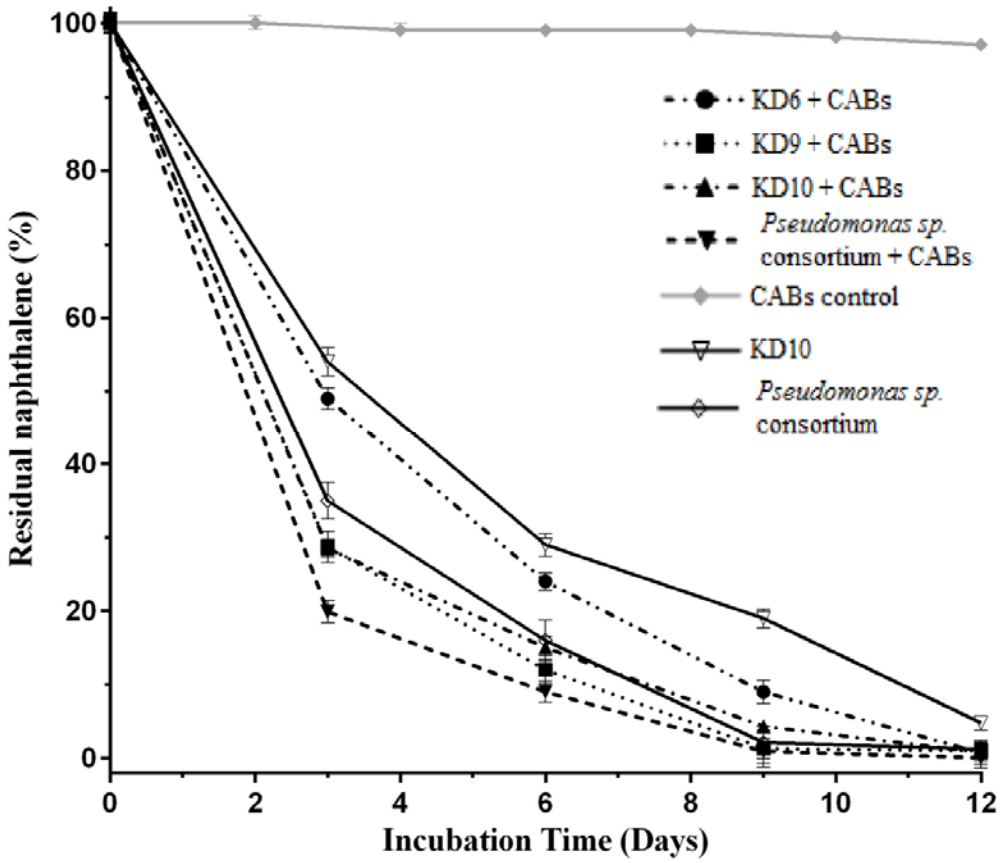
Residual naphthalene (%)
Incubation Time (Days)
KD6 + CABs
KD9 + CABs
KD10 + CABs
Pseudomonas sp. consortium + CABs
CABs control
KD10
Pseudomonas sp. consortium

Figure 5.

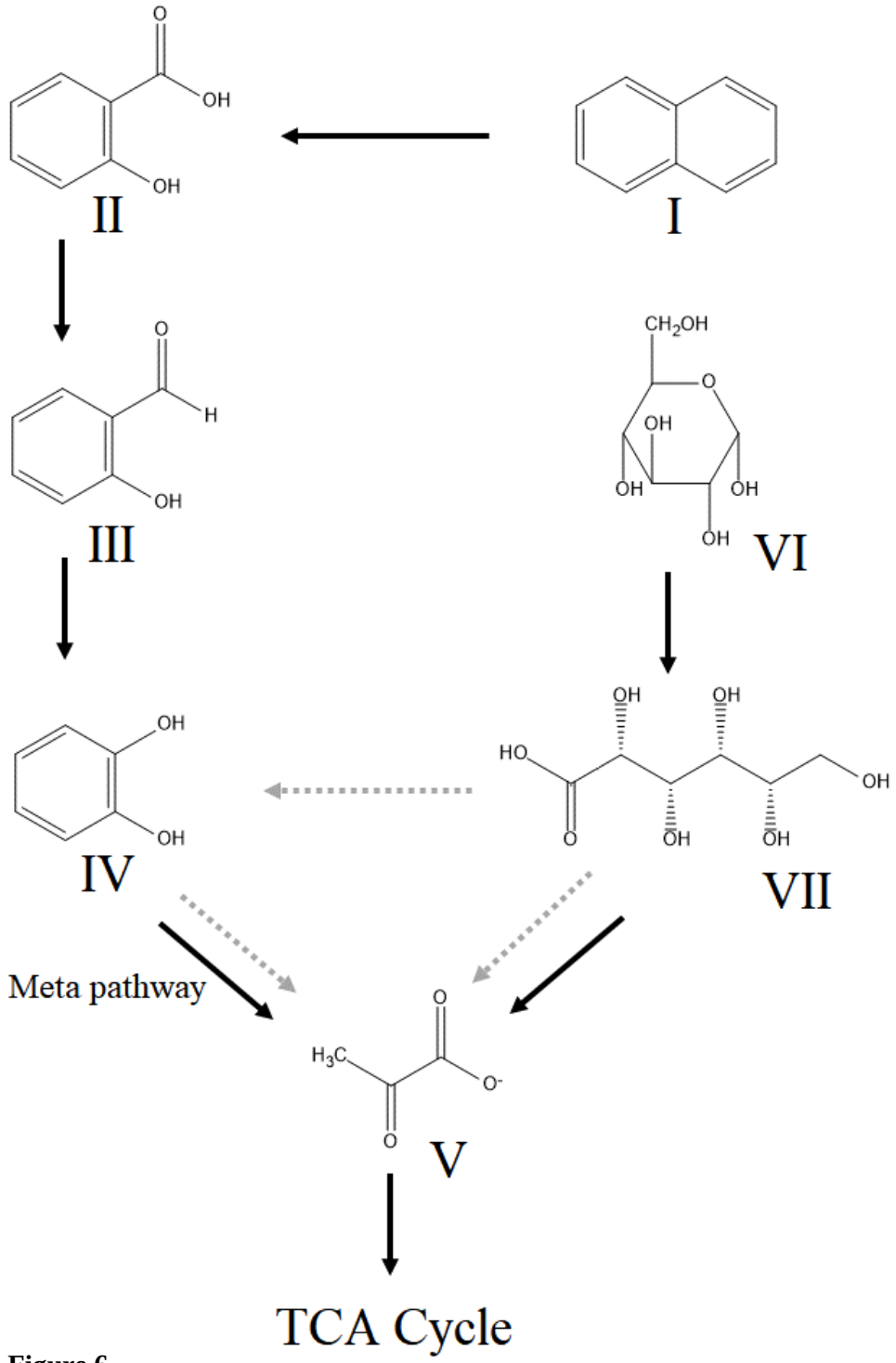
O
OH
OH
II
I
O
H
OH
III
CH2OH
O
OH
OH
OH
OH
VI
OH
OH
HO
OH
O
OH
OH
VII
OH
OH
IV
Meta pathway
O
H3C
O-
O
V
TCA Cycle

Figure 6.